# Non-innocent Ligand-Bridged Bimetallic Cyclometalated Iridium(III) Diastereomers for High-Efficiency Phosphorescent OLEDs[**]

*Yonghao Zheng, Andrei S. Batsanov, Mark A. Fox, Hameed A. Al-Attar, Khalid Abdullah, Vygintas Jankus, Martin R. Bryce* and Andrew P. Monkman*

***Abstract:*** *Phosphorescent dinuclear iridium(III) diastereomers (ΛΔ/ΔΛ) and (ΛΛ/ΔΔ) are readily separated by their different solubilities in hot hexane. The bridging diarylhydrazide ligand plays an important role in the electrochemistry and photophysics of the complexes. Organic light emitting devices (OLEDs), using these complexes as the green emissive dopants in solution-processable single-active-layer architectures, have remarkably high electroluminescence efficiencies for dinuclear metal complexes achieving maximum values of 37 cd $A^{-1}$, 14 lm $W^{-1}$ and 11% external quantum efficiency.*

**E**mitters with high luminous efficiency are essential for full-color organic light-emitting diode (OLED) displays[1] and white light sources.[2] Phosphorescent heavy metal complexes provide high electroluminescence (EL) efficiencies by harvesting both singlet and triplet electrogenerated excitons in the emitting layer.[1b, 3-5] Cyclometalated iridium(III) complexes are widely exploited because of their excited state lifetimes on the microsecond time-scale, high quantum yields, good thermal and chemical stability and tunability of emission color.[6-10] In this context the prototype complex is *fac*-Ir(ppy)$_3$ (ppy = 2-phenylpyridine).

The photoluminescence quantum yields of *dinuclear* metal complexes[11-25] are usually considerably lower than mononuclear analogs[12,14,23,24] (although there are exceptions)[25] leading to the established view that dinuclear complexes give poor device performance.[26,27] For example, the quantum yield of the bis($\mu$-Cl) bridged dimer [Ir(ppy)$_2$Cl]$_2$ **1** is only 0.5%,[11] whereas *fac*-Ir(ppy)$_3$ is 40(±0.1)% (both in toluene).[28] Consequently, the vast majority of phosphorescent OLED (PhOLED) studies have used mononuclear complexes.[1b] However, dinuclear complexes are attractive as their luminescence properties can be tuned by variation of the bridge and the cyclometalated ligands.[29]

Varying the bridging ligands to provide new diiridium systems is a largely unexplored topic. We now report the new diastereomeric complexes **3** and **4** and establish that the two diastereomers **3** (ΛΔ/ΔΛ) and **4** (ΛΛ/ΔΔ)) can be readily separated. Using complex **4** as the dopant in a simple solution-processed PhOLED architecture gave efficiencies of 37 cd $A^{-1}$, 14 lm $W^{-1}$ and 11% external quantum efficiency. To the best of our knowledge these are the highest reported efficiencies for PhOLEDs using a bimetallic complex as the emitter.

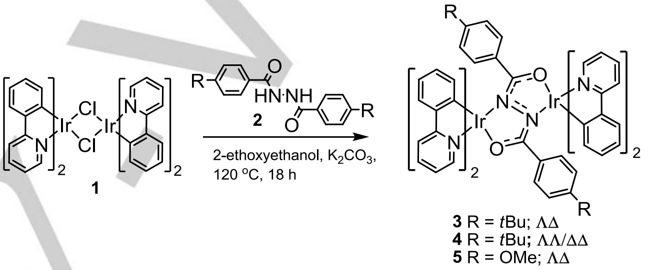

***Scheme 1.*** Synthesis of the complexes **3** - **5**.

Reaction of **1**[28] with **2** gave two diastereomers **3** (ΛΔ/ΔΛ 41% yield) and **4** (ΛΛ/ΔΔ 30% yield) (Scheme 1, Chart S1) which were readily separated by their different solubilities in hot hexane. The dimethoxy analog **5** (ΔΛ 43% yield) was similarly obtained and is included here due to the higher precision of its crystal structure compared to **3**. The structures of **3**-**5** were established by $^1$H NMR spectroscopy, mass spectrometry, elemental analysis and single crystal X-ray diffraction. There are two unique ppy groups in **3**, **4** and **5** as shown in the aromatic regions of their $^1$H NMR spectra (Figures 1, S1, S3 and S5). The peaks for two different pyridine rings (A and B) and the two phenylene rings (C and D) are assigned with the aid of $^1$H-$^1$H 2D COSY spectra (Figures S2 and S4). While there are studies[21,22,31] on enantiomer separation of monoiridium complexes, *facile separation of diastereomers of a diiridium complex into their pure forms like* ***3*** *and* ***4*** *has, to our knowledge, not been demonstrated previously*.

The electrochemical properties of **3** and **4** were examined by cyclic voltammetry in dichloromethane (DCM) solutions. The complexes show two reversible oxidation waves assigned to the formally Ir(III)/Ir(IV)-based processes at $E_{1/2}^{ox}$ 0.22 and 0.62 V (versus FcH/FcH$^+$, Figure S6 and Table S1) with peak splitting on the oxidative and reductive scans in the range 75 - 90 mV. The appearance of two waves separated by ca. 400 mV is consistent

---

[*] Dr. Y. Zheng, Dr. A. S. Batsanov, Dr. M. A. Fox, Prof. M. R. Bryce
Department of Chemistry, Durham University, Durham DH1 3LE (UK)
E-mail: m.r.bryce@durham.ac.uk

Dr. H. A. Al-Attar, K. Abdullah, Dr. V. Jankus, Prof. A. P. Monkman
Department of Physics, Durham University, Durham DH1 3LE (UK)

[**] We thank EPSRC for funding and Dr E. Pohl for access to the Bruker MicroStar rotating anode.

Supporting information for this article is available on the WWW under http://dx.doi.org/

with the involvement of the bridge in the first oxidation process as the two Ir…Ir centers are 5.1 Å apart.

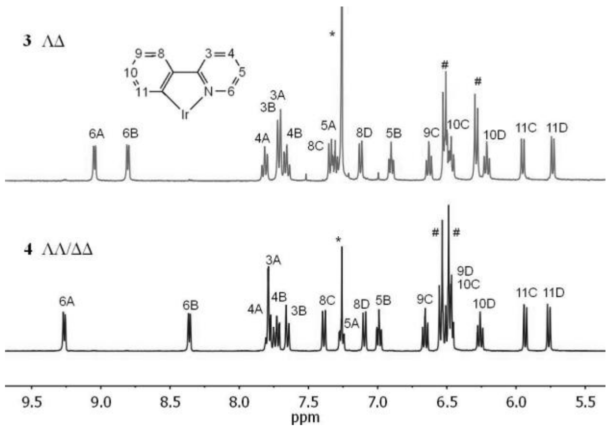

***Figure 1.*** Aromatic regions in the $^1$H NMR spectra for **3** and **4.** Peaks marked * are from residual $CHCl_3$ in $CDCl_3$ and peaks marked # are assigned to the aromatic protons of the *t*$BuC_6H_4$ group.

The crystal structure of **3** gives ΛΔ configuration for independent molecules *A* and *B* (Figure 2). As the precision was limited by the crystals' quality, the structure (ΛΔ) of analogue **5** (Figure S7) was also determined. The crystal of **4** contains inversion-related ΔΔ (Figure 2) and ΛΛ isomers, the molecule having approximate local $C_2$ symmetry but no crystallographic symmetry. The two linear N(py)-Ir-N(py) fragments are staggered by 59.3° in molecule **4**, but nearly parallel in **3** (to within 7.3° and 0.5°) and **5** (1.0°).[31]

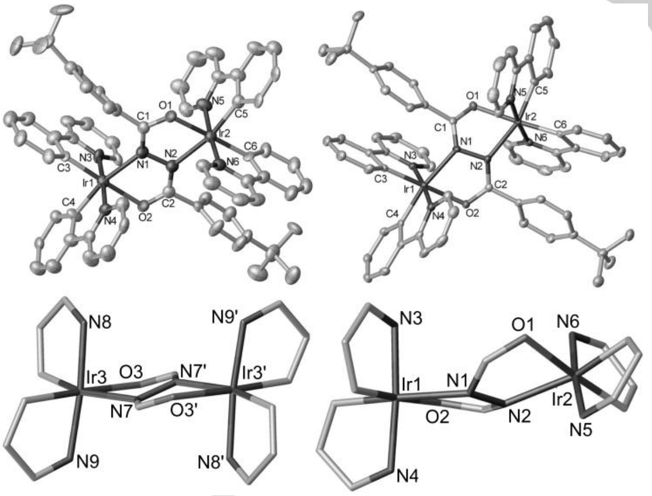

***Figure 2.*** X-ray molecular structures of **3** (left) (molecule *A*) and **4** (right). Primed atoms are generated by an inversion center. Thermal ellipsoids are drawn at 50% probability level, H atoms are omitted for clarity. Core parts of **3** (left) (molecule *B*) and **4** (right) in the X-ray structures.

The computed frontier molecular orbitals for the optimized geometries of **3** and **4** reveal the HOMOs to be of bridge (49-50%) and metal character (36%) as expected from the large separation of the two oxidation waves in their CV data (Figures 3, S12 and S13; Tables S5-S7). The LUMOs are located at the ppy ligands. The bridge involvement in the HOMOs of **3** and **4** contrasts with the HOMO of **1** which is located on the metal and the phenylene unit of the ppy ligand. We are not aware of a previous computational study on diiridium complexes where the bridge is heavily involved in the HOMO: typically the LUMO involves bridge character[16,18,23,32] or the bridge is not involved in either frontier orbital.[19,24]

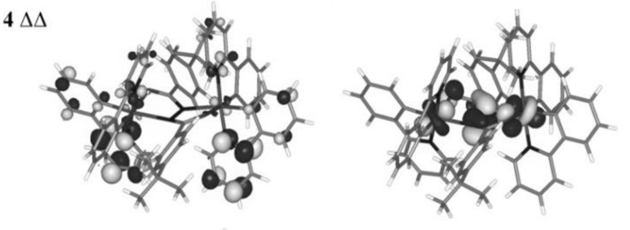

| LUMO -1.32 eV | HOMO -4.62 eV |
|---|---|
| Py : Ph : Ir : bridge | Py : Ph : Ir : bridge |
| 70 : 24 : 6 : 1 | 4 : 10 : 36 : 50 |

***Figure 3.*** Frontier orbitals for the optimized geometry of **4**.

The photophysical data for **2**, **3** and **4** are shown in Figures S8 and S9, Tables S3 and S4; data for $Ir(ppy)_3$ and **1** obtained under directly comparable conditions are included for comparison. The PL emissions of **3** and **4** at 521 nm and 523 nm are featureless which indicates a dominant $^3$MLCT contribution and little signature of $^3$LC contribution. The luminescence quantum yields of **3** and **4** in DCM solutions are 71% and 88%, whereas blended in zeonex at 5% w/w concentration the values are 38% and 41%, respectively. These are unusually high quantum yields for diiridium complexes and are comparable to $Ir(ppy)_3$ [40% in both DCM (this work) and in toluene.[28] The phosphorescence decays of **3** and **4** doped in zeonex at 5% (Figure S10) show very similar lifetimes to $Ir(ppy)_3$ (ca. 1.4 $\mu$s) consistent with emission from a triplet excited state. The emission of **3** and **4** in DCM solution ($\lambda_{max}$ 521-523 nm) is red shifted compared to $Ir(ppy)_3$ (510 nm).

Devices were fabricated by spin-coating to give the single-active-layer structure: ITO/PEDOT:PSS (50 nm)/[PVK:PBD (40%):Ir complex (5%)] (90 nm)/Ba(4 nm)/Al(100 nm). Figures 4 and S14-S16 show the device characteristics for complexes **1**, **3** and **4**. Figures 4, S16 and Table 1 also include data for the previously reported bis(μ-Cl) bridged diiridium complex where the C^N ligands are cyclometalated fluorenylpyridine (flpy), [Ir(flpy)$_2$Cl]$_2$ (Chart S2).[24] This complex is compared as it has similar solubility to complex **4**. Complex **4** displays very high performance, with EQE 11% and current efficiency 37 cd/A, compared to 7% and 24 cd/A for **3**. To our knowledge these values for **4** are the best reported to date for solution-processed devices of diiridium complexes and they are significantly higher than the previous highest values of 4% and 12 cd/A reported for Ir$_2$(flpy)$_4$Cl$_2$ (2.5% and 8.5 cd/A under the same conditions as devices **3** and **4**).[24] The enhanced device efficiency of complex **4** compared to **3** may be explained by the increased solubility of **4** and the different film morphologies based on the different molecular conformations of **3** and **4** (Figure 2). We note that *complex **4** has even higher device efficiency than the benchmark green emitter Ir(ppy)$_3$ at dopant concentration of 5% for a single-active-layer solution processed device.*[33]

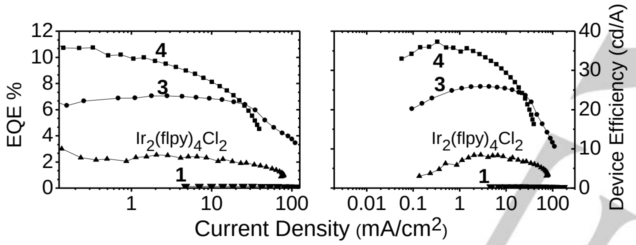

***Figure 4.*** Device characteristics for 5% w/w dopant concentration of complexes **1**, **3**, **4** and [Ir(flpy)$_2$Cl]$_2$. Data for [Ir(flpy)$_2$Cl]$_2$ are taken from ref. 25.

***Table 1.*** Turn-on voltage and maximum device efficiencies for **1, 3**, **4** and [Ir(flpy)$_2$Cl]$_2$.

| Complex | Turn-on voltage (V) at 1 cd/m$^2$ | EQE % | Current efficiency (cd/A) | Maximum brightness (cd/m$^2$) | Power efficiency (lm/W) | Maximum radiant power (mW) |
|---|---|---|---|---|---|---|
| **1** | 8 | 0.15 | 0.35 | 220 | 0.12 | 0.05 |
| **3** | 6.2 | 7 | 24 | 11,000 | 7 | 0.8 |
| **4** | 5.5 | 11 | 37 | 7,000 | 14 | 1.8 |
| *fac*-[Ir(flpy)$_2$Cl]$_2$ (ref. 25) | 4.7 | 2.5 | 8.5 | 3,000 | 3 | 0.4 |

To probe the reasons for high efficiency in these diiridium PhOLEDs, the EL transient of the device ITO/PEDOT-PSS/[PVK: 40% PBD: 5% complex **3**]/Ba/Al was compared with the photoluminescence (PL) transient (Figure S18a). The first feature lasting from 0.1 μs to 10 μs is a single exponential with a lifetime of ca. 1.4 μs, and the second lasting from 10 μs to 1 ms is a power law with the slope ca. -0.6. Time resolved spectra (Figure S18b) recorded between 900 - 1500 ns (during exponential decay) and between 140 -160 μs (during the power law decay) are identical indicating that both features arise due to the same emissive state of **3**. The lifetime of the emissive state is only 1.45 μs (Table S4) thus at later times it must be fed from another state thereby substantially increasing the EL. To the best of our knowledge *similar power law features in iridium based PLEDs have not been reported previously*.

In conclusion, three special features of this work are: i) the two diastereomeric complexes **3** (ΛΔ/ΔΛ) and **4** (ΛΛ/ΔΔ) are readily separated; ii) the bridging ligands are non-innocent; iii) complex **4** gives green PhOLEDs with efficiencies of 37 cd A$^{-1}$, 14 lm W$^{-1}$ and 11% EQE which are remarkably high for dinuclear metal complexes. There is considerable scope for exploring new diiridium complexes, especially with conjugated or non-innocent bridging ligands, to probe interactions between the metal centers, achieve color tuning and to obtain highly efficient OLEDs.

**Keywords:** Iridium; ligand design; diastereomer; luminescence; organic light-emitting devices

---

[1] a) *Organic Light-Emitting Devices* (Eds.: K. Müllen, U. Scherf), Wiley-VCH, Weinheim, **2006**; b) *Highly Efficient OLEDs with Phosphorescent Materials* (Ed.: H. Yersin), Wiley-VCH, Weinheim, Ch 8, **2008**; c) S. Y. Lee, T. Yasuda, Y. S. Yang, Q. Zhang, C. Adachi, *Angew. Chem. Int. Ed.* **2014**, *53*, 6402–6406.

[2] a) Review: K. T. Kamtekar, A. P. Monkman, M. R. Bryce, *Adv. Mater.* **2010**, *22*, 572–582; b) W-X. Ni, M. Li, J. Zheng, S-Z. Zhan, Y-M. Qiu, S. W. Ng, D. Li, *Angew. Chem. Int. Ed.* **2013**, *52*, 13472–13476.

[3] M. A. Baldo, D. F. O'Brien, Y. You, A. Shoustikov, S. Sibley, M. E. Thompson, S. R. Forrest, *Nature* **1998**, *395*, 151–154.

[4] Y. Kawamura, K. Goushi, J. Brooks, J. J. Brown, H. Sasabe, C. Adachi, *Appl. Phys. Lett*. **2005**, *86*, 071104.

[5] X-C. Hang, T. Fleetham, E. Turner, J. Brooks, J. Li, *Angew. Chem. Int. Ed*. **2013**, *52*, 6753–6756.

[6] S. Lamansky, P. Djurovich, D. Murphy, F. Abdel-Razzaq, H-E. Lee, C. Adachi, P. E. Burrows, S. R. Forrest, M. E. Thompson, *J. Am. Chem. Soc.* **2001**, *123*, 4304–4312.

[7] Review: E. Holder, B. M. W. Langeveld, U. S. Schubert, *Adv. Mater*. **2005**, *17*, 1109–1121.

[8] Review: L. Xiao, Z. Chen, B. Qu, J. Luo, S. Kong, Q. Gong, J. Kido, *Adv. Mater*. **2011**, *23*, 926–952.

[9] N. Tian, D. Lenkeit, S. Pelz, D. Kourkoulos, D. Hertel, K. Meerholz, E. Holder, *Dalton Trans*. **2011**, *40*, 11629–11635.

[10] D. Xia, B. Wang, B. Chen, S. Wang, B. Zhang, J. Ding, L. Wang, X. Jing, F. Wang, *Angew. Chem. Int. Ed.* **2014**, *53*, 1048–1052.

[11] G. A. Carlson, P. I. Djurovich, R. J. Watts, *Inorg. Chem.* **1993**, *32*, 4483–4484.

[12] A. Tsuboyama, T. Takiguchi, S. Okada, M. Osawa, M. Hoshino, K. Ueno, *Dalton Trans.* **2004**, 1115–1116.

[13] E. A. Plummer, J. W. Hofstraat, L. De Cola, *Dalton Trans*. **2003**, 2080–2084.

[14] A. Santoro, A. M. Prokhorov, V. N. Kozhevnikov, A. C. Whitwood, B. Donnio, J. A. G. Williams, D. W. Bruce, *J. Am. Chem. Soc.* **2011**, *133*, 5248–5251.

[15 ] V. Chandrasekhar, S. M. W. Rahaman, T. Hajra, D. Das, T. Ghatak, S. Rafiq, P. Sen, J. K. Bera, *Chem. Commun*. **2011**, *47*, 10836–10838.

[16 ] E. S. Andreiadis, D. Imbert, J. Pécaut, A. Calborean, I. Ciofini, C. Adamo, R. Demadrille, M. Mazzanti, *Inorg. Chem.* **2011**, *50*, 8197–8206.

[17 ] E. Baranoff, E. Orselli, L. Allouche, D. Di Censo, R. Scopelliti, M. Gratzel, M. D. Nazeeruddin, *Chem. Commun*. **2011**, *47*, 2799–2801.

[18] V. Chandrasekhar, T. Hajra, J. K. Bera, S. M. W. Rahaman, N. Satumitra, O. Elbjeirami, M. A. Omary, *Inorg. Chem*. **2012**, *51*, 1319–1329.

[19] V. Chandrasekhar, B. Mahanti, P. Bandipalli, K. Bhanuprakash, *Inorg. Chem*. **2012**, *51*, 10536−10547.

[20] V. L. Whittle, J. A. G. Williams, *Inorg. Chem*. **2008**, *47*, 6596–6607.

[21] A. Auffrant, A. Barbieri, F. Barigelletti, J. Lacour, P. Mobian, J-P. Collin, J-P. Sauvage, B. Ventura, *Inorg. Chem*. **2007**, *46*, 6911–6919.

[22] M. Graf, R. Czerwieniec, K. Sünkel, *Z. Anorg. Allg. Chem*. **2013**, *639*, 1090–1094.

[23] L. Donato, C. E. McCusker, F. N. Castellano, E. Zysman-Colman, *Inorg. Chem*. **2013**, *52*, 8495–8504.

[24] A. M'hamedi, A. S. Batsanov, M. A. Fox, M. R. Bryce, K. Abdullah, H. A. Al-Attar, A. P. Monkman, *J. Mater. Chem*. **2012**, *22*, 13529–13540.

[25] P-H. Lanoe, C. M. Tong, R. W. Harrington, M. R. Probert, W. Clegg, J. A. G. Williams, V. N. Kozhevnikov, *Chem. Commun*. **2014**, *50*, 6831–6834.

[26] S. Bettington, M. Tavasli, M. R. Bryce, A. S. Batsanov, A. L. Thompson, H. A. Al Attar, F. B. Dias, A. P. Monkman, *J. Mater. Chem*. **2006**, *16*, 1046–1052.

[27] X. Li, D. Zhang, W. Li, B. Chu, L. Han, T. Li, Z. Su, J. Zhu, Y. Chen, Z. Hu, P. Lei, Z. Zhang, *Optical Materials* **2009**, *31*, 1173–1176.

[28] K. A. King, P. J. Spellane, R. J. Watts, *J. Am. Chem. Soc*. **1985**, *107*, 1431–1432.

[29] V. W-W. Yam, K. M-C. Wong, *Chem. Commun*. **2011**, *47*, 11579–11592.

[30] a) C. Schnaffner-Hamann, A. von Zelewsky, A. Barbieri, F. Barigelletti, G. Muller, J. P. Riehl, A. Neels, *J. Am. Chem. Soc.* **2004**, *126*, 9339–9348; b) C. Hamann, A. von Zelewsky, A. Neels, H. Stoeckli-Evans, *Dalton Trans.* **2004**, 402–406; c) F. J. Coughlin, M. S. Westrol, K. D. Oyler, N. Byrne, C. Kraml, E. Zysman-Colman, M. S. Lowry, S. Bernhard, *Inorg. Chem.* **2008**, *47*, 2039–2048; d) E. Marchi, R. Sinisi, G. Bergamini, M. Tragni, M. Monari, M. Bandini, P. Ceroni, *Chem. Eur. J.* **2012**, *18*, 8765–8773.

[31] CCDC 995196 (complex **3**), 995198 (complex **4**) and 995197 (complex **5**) contain the crystallographic data for this paper. These data can be obtained free of charge from The Cambridge Crystallographic Data Centre via www.ccdc.cam.ac.uk/data_request/cif.

[32] A. M. Soliman, D. Fortin, P. D. Harvey, E. Zysman-Colman, *Dalton Trans.* **2012**, *41*, 9382–9393.

[33] H. A. Al-Attar, G. C. Griffiths, T. N. Moore, M. Tavasli, M. A. Fox, M. R. Bryce, A. P. Monkman, *Adv. Funct. Mater.* **2011**, *21*, 2376–2382.

## Table of Contents

## COMMUNICATION

The phosphorescent dinuclear iridium(III) diastereomers (see picture) are readily separated. The bridging diarylhydrazide ligand plays an important role in the electrochemistry and photophysics of the complexes. OLEDs using these complexes as green emissive dopants have remarkably high electroluminescence efficiencies for dinuclear metal complexes, achieving 37 cd A$^{-1}$, 14 lm W$^{-1}$ and 11% external quantum efficiency in a simple device architecture.

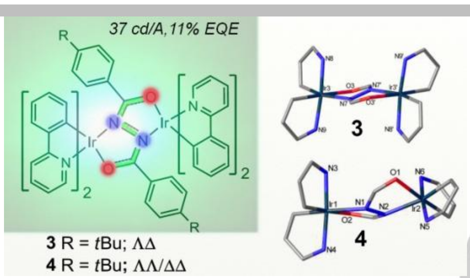

*Yonghao Zheng, Andrei S. Batsanov, Mark A. Fox, Hameed A. Al-Attar, Khalid Abdullah, Vygintas Jankus, Martin R. Bryce* and Andrew P. Monkman*

***Page No. – Page No.***

**Non-innocent Ligand-Bridged Bimetallic Cyclometalated Iridium(III) Diastereomers for High-Efficiency Phosphorescent OLEDs**